Electronic Supplementary Material (ESI) for CrystEngComm.

Photorefraction of uranium-doped lithium niobate crystals at multiple visible wavelengths

Tian Tian, [a] *Yuheng Chen,* [a] *Jie Zhang,* [a] *Shuolin Wang,* [b] *Wen Yuan,* [a] *Hongde Liu,* [*c] *Yaoqing Chu,* [a] *Chengling Mao,* [a] *Wenjie Xu,* [a] *Dahuai Zheng,* [c] *and Jiayue Xu* [*a]

[a] Institute of Crystal Growth, School of Materials Science and Engineering, Shanghai Institute of Technology, Shanghai 201418, China.

[b] School of Science, Jiangsu University of Science and Technology, Zhenjiang 212100, China.

[c] MOE Key Laboratory of Weak-Light Nonlinear Photonics, School of Physics and TEDA Institute of Applied Physics, Nankai University, Tianjin 300071, China.

*E-mail: liuhd97@nankai.edu.cn; xujiayue@sit.edu.cn.

Contents

Solid State Syntheses.

LN: U polycrystalline powder was synthesized by high temperature solid phase sintering method. Li_2CO_3 (99.99%) and Nb_2O_5 (99.99%) and high purity UO_2 as raw materials, according to the ratio of [Li]/[Nb] = 48.38/51.62, after fully grinding and mixing, the polycrystalline powder was put into a corundum crucible and placed in a high-temperature muffle furnace at 1200 °C for sintering. The temperature was raised to 800 °C and kept for 5 h, then was raised to 1100 °C and kept for 7 h. Finally, the temperature naturally cooled down to room temperature to obtain LN: U polycrystalline material.

Crystal growth.

We first placed a pure congruent LN crystal (CLN) seed crystal with a diameter of 1 cm at the bottom of a platinum crucible, whose diameter is 1 inch in the equal diameter part. Then, taken out the prepared polycrystalline material, put them into the platinum crucible, and placed it in an alumina insulation tube after sealing. The alumina powder was selected as the insulation material, to maintained a stable thermal field, and finally placed in the growth furnace. In order to fully melt the raw materials, the polycrystalline powder was heated by medium-frequency induction and kept above the melting point of 100 °C for 2–3 h. Both CLN and LN: U crystals were grown along the c axis. The descending rate were controlled at 0.3–0.4 mm/h. The vertical temperature gradient above the solid-melt interface was about 0.3–0.4 °C/mm measured by thermocouple. As grown LN: U crystal are shown in Figure S1. Crystals

were polarized at an electric current density of 7 mA / cm^2 for 20 min at 1190 ℃ to form a single-domain structure. The 1 mm and 3 mm thick wafers were cut and polished to the optical grade for subsequent performance testing.

Powder X-ray diffraction.

Powder X-ray diffraction (XRD) were performed on D/Max-RA (Rigaku, Japan) with a test range of 20–70◦, at 40 kV and 20 mA (λ = 1.5418 Å).

Structure determination.

The crystal structure was solved by direct methods in TOPAS academic system and the structure was refined by Rietveld method to check for missing structures. The crystal structure parameters were shown in Table S1.

Crystalline quality.

The high-resolution X-ray rocking curve of Bruker HRXRD-5000 was used to test 1.0 mm thick samples to characterize the crystalline quality of LN: $U_{2.0}$ crystals. The rocking curves were shown in Figure S2.

Holographic experiment.

The PR properties of LN: U were measured by two-wave coupling method in transmission geometry using continuous wave (CW) lasers at wavelengths of 488 nm (Ar^+ laser), 532 nm and 671 nm (frequency-doubled solid-state lasers) in a traditional holographic setup. Two mutually coherent beams irradiated these 3.0 mm thick crystal at a cross angle of 30°, the grating vector formed by the two beams in the crystal is along the c-axis to obtain the maximum electro-optic coefficient r_{33}. The

diffraction efficiency measured in the experiment was defined as $\eta = I_d / (I_d+I_t)$, where I_d and I_t are the diffraction and transmission beam intensity, respectively. By fitting the function $\eta(t) = \eta_s [1 - \exp(-t/\tau_r)]^2$ to the data, the PR response time constant τ_r and the saturation diffraction efficiency η_s were derived. The refractive index change Δn was calculated according to the Kogelnik's coupled wave theory, followed from $\Delta n = [\lambda \cos\theta / (\pi d)] \arcsin\sqrt{\eta_S}$, where λ is the wavelength in vacuum, θ is the half crossing angle of the two writing beams in crystal, and d is the crystal thickness.[31] In order to express the PR performances comprehensively, the photorefractive sensitivity $S = (d\sqrt{\eta_S} / dt)_{t=0} / (Id)$ was used to characterize its performance. In the above formula, I is the total recording light intensity and d is the crystal thickness. The optical circuit diagram of dual-wave coupling experiment was shown in Figure S3, and the writing curves of LN: $U_{0.6}$ at different wavelengths were shown in Figure S4.

Determination method of the photorefractive dominant carrier type and carrier migration mechanism.

The dominant carrier type and carrier migration mechanism in LN could also be confirmed by light amplification with the same set up in holographic experiment. The intensity ratio between the transmitted light intensities of S beam and R beam was set as 1:1. During the process of recording the phase grating, if there is a stable energy transfer between the two beams which named the optical amplification, it indicates that the diffusion effect dominates the photorefraction process. And the light

energy transfer toward −c axis means the dominant carriers are electrons, while the light energy transfer toward +c axis for holes.

UV–Visible absorption spectra.

The UV-Visible absorption spectra of LN: U were measured at room temperature by a Cary - 5000 spectrophotometer within wavelength range of 300 - 800 nm and step length of 0.5 nm.

Figure S1. LN: U crystal were grown by the modified vertical Bridgman method, from bottom to top were LN: $U_{0.3}$, LN: $U_{0.6}$, LN: $U_{1.0}$ and LN: $U_{2.0}$, respectively.

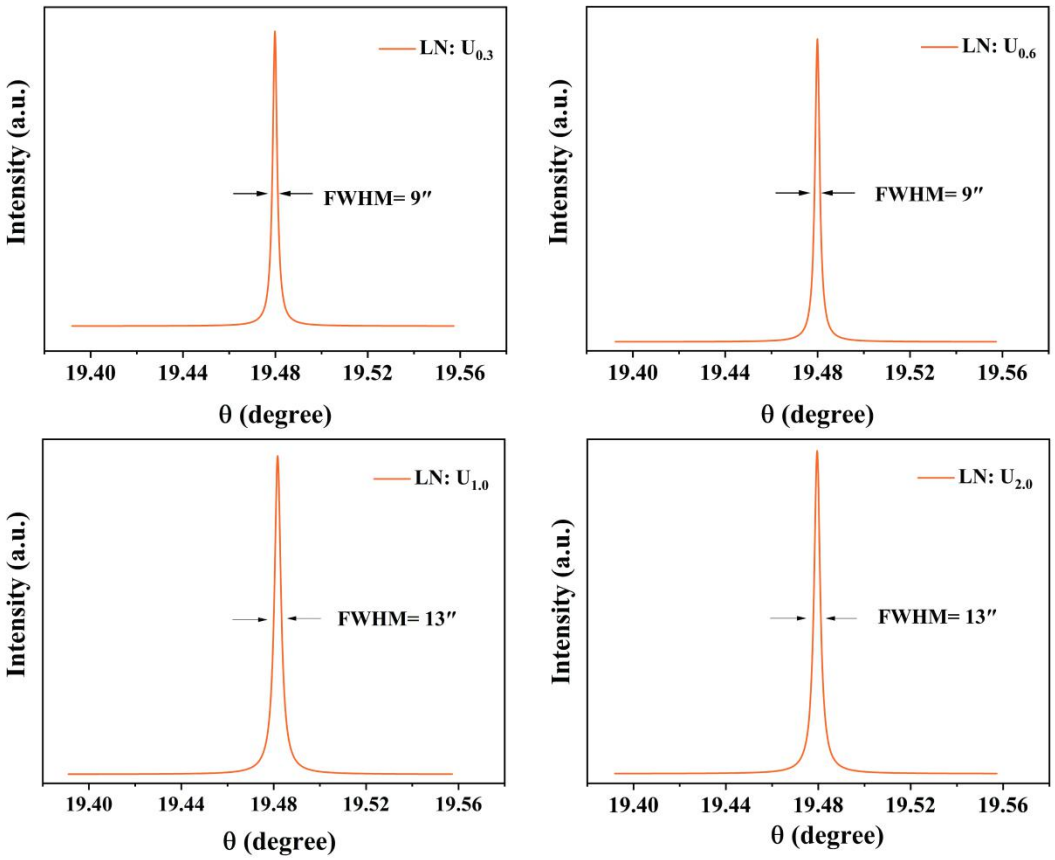

Figure S2. X-ray rocking curves of LN: $U_{0.3}$, LN: $U_{0.6}$, LN: $U_{1.0}$ and LN: $U_{2.0}$ crystals in (001) direction.

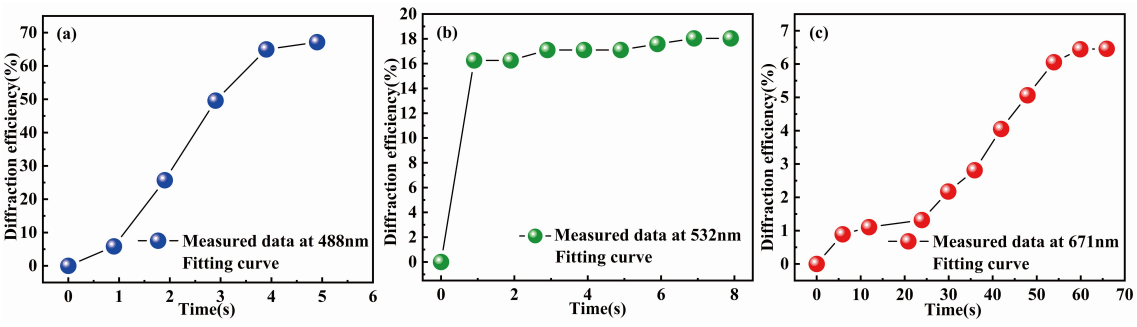

Figure S3. Holographic writing curves of LN: $U_{0.6}$ at different visible wavelengths.

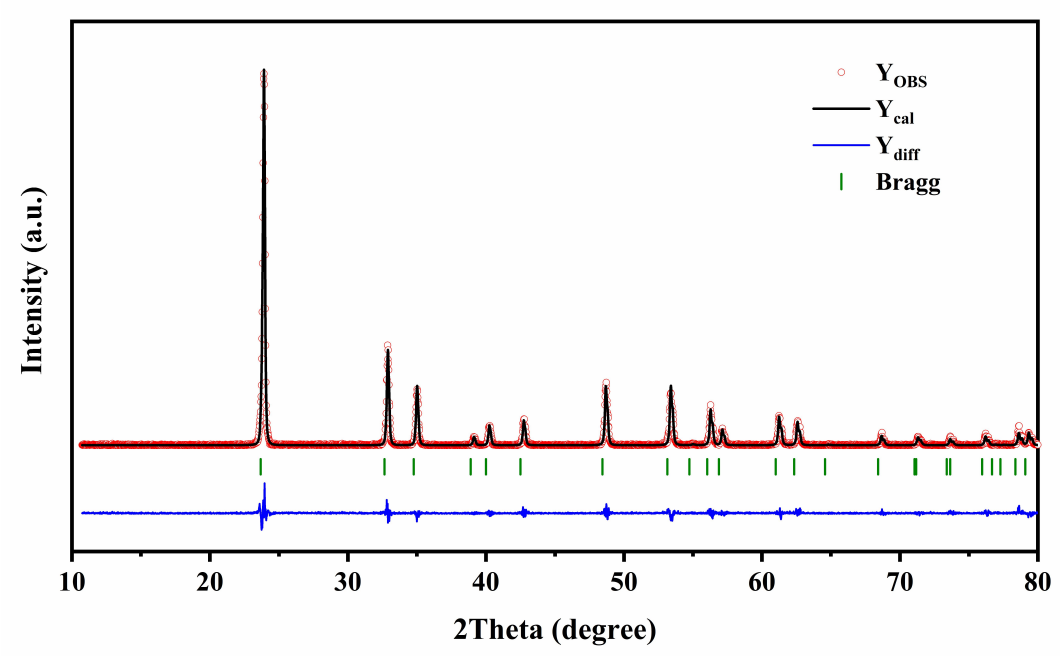

Figure S4. Rietveld refinement of powder XRD pattern of LN: $U_{2.0}$.

Table S1. Crystallographic data of LN:$U_{2.0}$.

Formula	LN:$U_{2.0}$
Crystal system	trigonal system
Space-group	R3c
a(Å)	5.15618(16)
b(Å)	5.15618(16)
c(Å)	13.88182(57)
α(°)	90
β(°)	90
γ(°)	120
Volume(Å^3)	319.619(24)